

## EXPERIMENTAL STUDY OF OSCILLATING SD8020 FOIL FOR PROPULSION

S. Srigrarom, W.S. Chai and H.T. Tan

School of Mechanical and Aerospace Engineering  
 Nanyang Technological University, Singapore, 639798, SINGAPORE

### Abstract

The thrust producing performance and efficiency of an SD8020 oscillating foil with a symmetrical saw-tooth angle of attack pitching profile was studied through force and torque measurements, as well as dye flow visualization, in the water tunnel at low Reynolds number of 13,000-16,000. The propulsive efficiency and thrust coefficient of the pitching foil were determined as a function of the Strouhal number, pitch amplitude and angular frequency. A propulsive efficiency of 30% was obtained experimentally at low Strouhal numbers. The flow visualization has revealed different wake patterns at various Strouhal numbers and can be classified into three regimes – a drag wake, a transition wake and a thrust wake. The drag wake consists of a combination of a regular Kármán street and an array of ‘primary’ stop-start vortices, whereas the thrust wake consists of a reverse Kármán vortex street, commonly observed in swimming fish. The transition wake regime, which occurs at approximately  $0.2 < St < 0.5$ , is interpreted as a momentum balanced wake, where the thrust developed by the foil approximately balances its produced drag. This wake was observed to either consist of an inclined vortex street, or a paired vortex pattern. Based on the force and efficiency data collected, increasing pitch amplitude and angular frequency was associated with a decrease in propulsive efficiency and an increase in thrust forces produced. A high efficiency value of 0.3, accompanied by a thrust coefficient of order one is found at a low pitch amplitude of  $10^\circ$ , angular frequency of 0.79 rad/s and Strouhal number of 0.05. This presented the best conditions for thrust production observed at low Strouhal and Reynolds numbers.

### Introduction

The purpose of this project is to study the flapping motions of airfoil (SD8020) in order to obtain a good flapping motion which can produce thrust and obtain a better power efficiency for the miniature under water vehicle propulsion system.

The experiment on the flapping airfoil in water tunnel was carried out as well as the flow visualization on the stationary and flapping airfoil. In the current study the pitching motion is saw-tooth like pattern with variable period and amplitude.

### Principal parameters of an oscillating foil

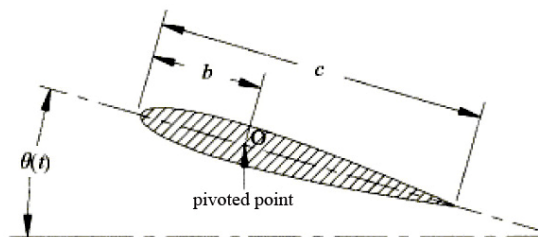


Fig.1: The parameter for flapping motion of airfoil.

Figure 1 shows a foil with chord length  $c$  and span  $s$ , moving at constant forward velocity  $U$  with an angular (pitch) motion,  $\theta(t)$ , of amplitude  $\theta_0$  and frequency  $\omega$ .

Under these conditions, the foil is subject to time-varying forces  $X(t)$  and  $Y(t)$  in the  $x$ - (forward, thrust or drag) and  $y$ - (transverse, or lift) directions, respectively, and a torque  $Q(t)$ . The foil is assumed to pitch about a point  $O$ , whose distance from the leading edge is denoted by  $b$ .  $T$  is the period of oscillation, following Triantafyllou's notation (Triantafyllou et al., 1991), we denote by  $F$  the time-averaged value of  $X(t)$ , and by  $P$  the average input power per cycle, i.e.

$$F = \frac{1}{T} \int_0^T X(t) dt \quad \text{and} \quad P = \frac{1}{T} \int_0^T Q(t) \frac{d\theta}{dt}(t) dt \quad (1)$$

The power coefficient  $C_p$  and the thrust coefficient  $C_T$  are:

$$C_p = \frac{P}{0.5\rho S_0 U^3} \quad \text{and} \quad C_T = \frac{F}{0.5\rho S_0 U^2} \quad (2)$$

where  $\rho$  denotes the fluid density, and  $S_0$  denotes the area of one side of the foil, i.e. for the rectangular foil used in this study, of chord  $c$  and span  $s$ ,  $S_0 = cs$ .

The propulsive efficiency,  $\eta_p$ , is defined to be the ratio of useful power over input power, as

$$\eta_p = \frac{FU}{P} \quad \text{and that} \quad \eta_p = \frac{C_T}{C_p} \quad (3)$$

The non-dimensional frequency, called the Strouhal number  $St$  is defined as

$$St = \frac{fA}{U} \quad \text{and} \quad A = 2(c-b) \sin \theta_{\max} \quad (4)$$

where  $f$  denotes the pitching frequency of foil oscillation in Hz, and  $A$  denotes the characteristic width of the created jet flow.

Since this is unknown before measurements are made,  $A$  is taken to be equal to double the wing swept area, as shown in (4), which is derived from figure 1.

### Experimental Results

The experiment was carried out in the low speed 45cm x 45cm water tunnel, as shown in figure 2. A symmetrical rigid airfoil (SD8020), as shown in figure 3, was used for the stimulation. The airfoil has span of 32cm and chord length of 12cm thickness at the pivot point is 1cm. The raised platform plate was added below the wing to keep the flow 2 dimensional.

The ATI Gamma 6-axis force/torque load cell and an 8SMC1-USBh motorized rotary stage to record and read the force on the airfoil and produce the pitching motion. The pitching pattern follow linear saw tooth motion, as shown in figure 4.

Force in  $x$ - direction ( $X$ ) was recorded by Load Cell and analysed with different pitching motion, flapping amplitude and water flow speed. The positive  $X$  value is *drag* and hence, the negative  $X$  is *thrust* force as the water flow is from the left side of the airfoil in Figure 2.

The Experiments was divided into two parts: Inspection of oscillation pattern with and without flow, and Summary of all force and efficiency tests. The first section will examine the case with and without free stream velocities, i.e.: zero (no freestream flow) and with freestream flow at  $U = 0.1028$  m/s. The graphs below show the force in  $x$ -direction vs. the time in m/s.

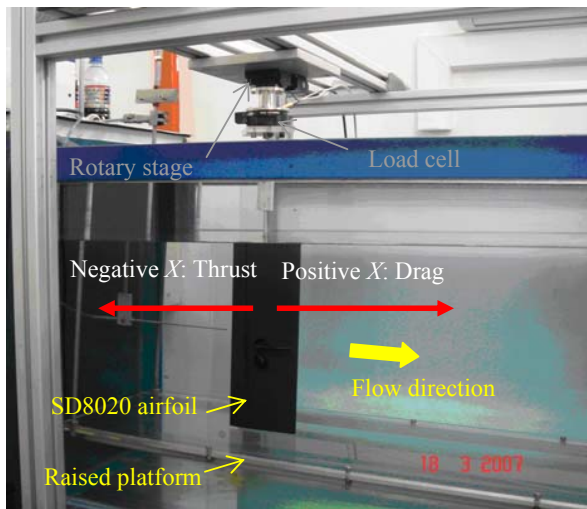


Figure 2: Experimental setup

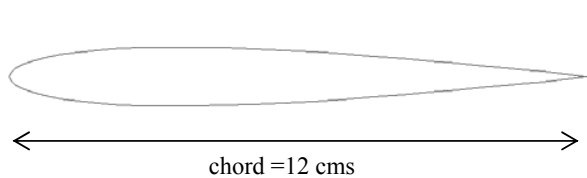


Figure 3: The SD8020 airfoil and its dimension.

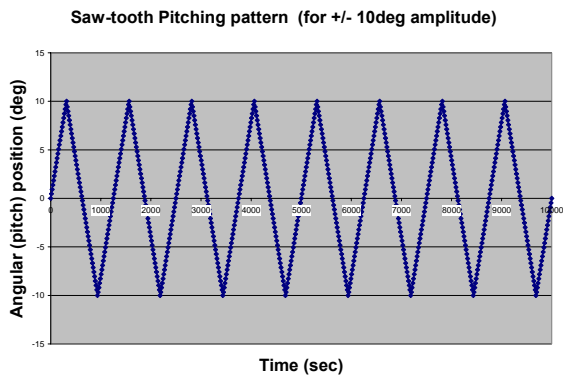


Figure 4: Linear saw-tooth like pitching pattern.

1. Zero flow speed (stationary airfoil), pitching rate at 40 deg per sec, and pitching amplitude = 10 deg

In this condition, the flapping airfoil caused only drag. The force recording is shown in figure 5. The forces ( $F_x = X(t)$ ,  $F_y = Y(t)$ ) and torque (moment) ( $T_z = Q(t)$ ) loci are shown in figures 6 and 7 respectively. The Thrust (drag) coefficient is found to be  $C_T = -0.068$ .

2. With freestream flow speed ( $U = 0.1028$  m/s), pitching rate at 40 deg per sec, and pitching amplitude = 10 deg

This case is similar to the previous one, except there is freestream flow ( $U = 0.1028$  m/s) past to it. The Strouhal number, as defined in (4), is  $St = 0.3243$ . The force recording is shown in figure 8. The forces ( $F_x = X(t)$ ,  $F_y = Y(t)$ ) and torque (moment) ( $T_z = Q(t)$ ) loci are shown in figures 9 and 10 respectively. In contrast to the previous case, there is thrust produced by this pitching airfoil. The thrust coefficient is found to be  $C_T = 0.145$ . The corresponding efficiency is  $\eta = 0.100$ .

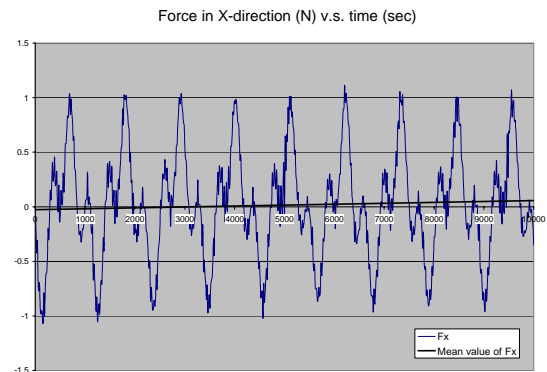


Figure 5: Reading of force in x-direction for zero flow, 40 deg/sec pitching rate and 10 deg amplitude.

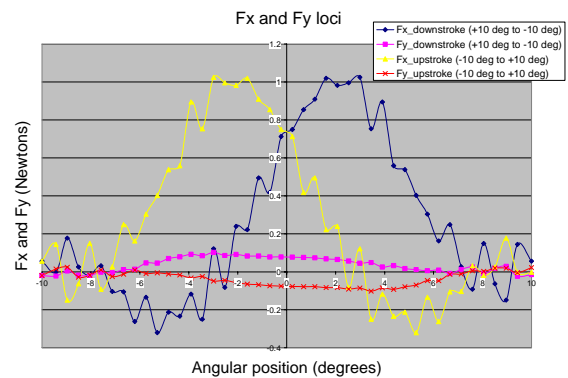


Figure 6: Forces loci for zero flow, 40 deg/sec pitching rate and 10 deg amplitude.

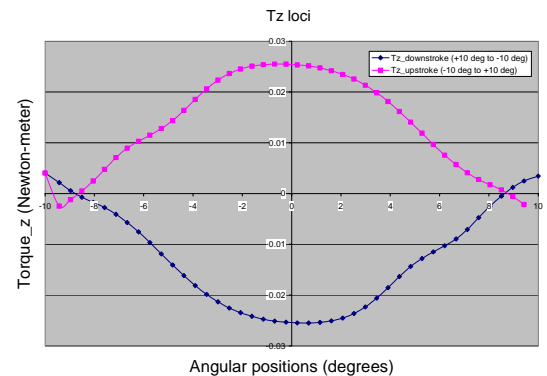


Figure 7: Torque loci for zero flow, 40 deg/sec pitching rate and 10 deg amplitude.

The sample dye flow visualization snap shot is shown in figures 11. The shed vortex pattern resembles jet flow, and hence, the airfoil under this flow condition is producing thrust. There is only one vortex shed from each stroke (either up or down).

The force reading and force loci in figures 8 and 9 show interesting feature. There is a saddle point or kink in each stroke (either up or down). This is caused by the vortex formed on the inside surface of the airfoil. This vortex creates vortex lift in opposite sense to the airfoil moving direction, and that, causes reduction in resultant force. Later, the vortex is shed downstream out of the airfoil into the wake. Hence the resultant force restored.

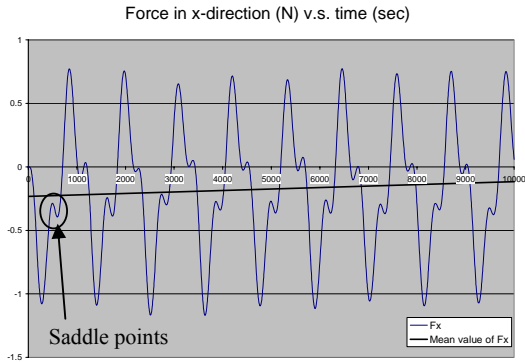


Figure 8: Reading of force in x-direction for  $U = 0.1028$  m/s flow, 40 deg/sec pitching rate and 10 deg amplitude.

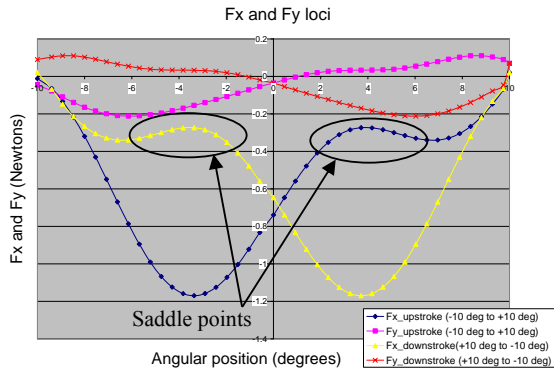


Figure 9: Forces loci for  $U = 0.1028$  m/s flow, 40 deg/sec pitching rate and 10 deg amplitude.

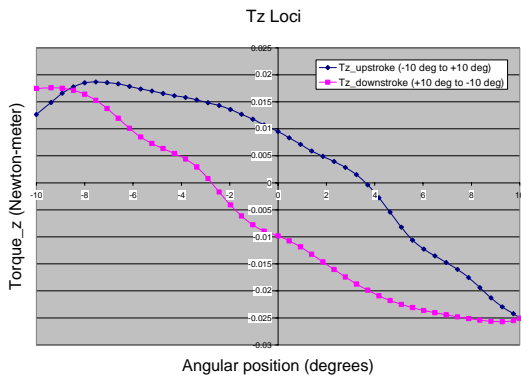


Figure 10: Torque loci ( $T_z = Q(t)$ ) for  $U = 0.1028$  m/s flow, 40 deg/sec pitching rate and 10 deg amplitude.

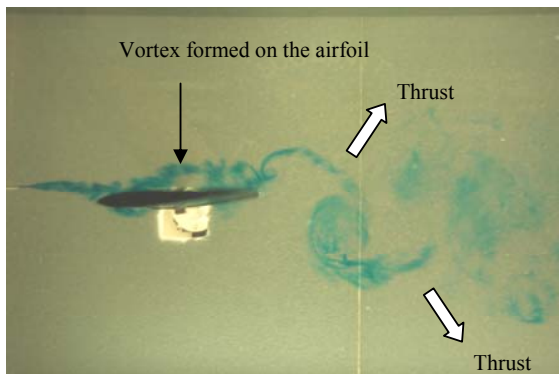


Figure 11: Dye flow visualization. The shed vortex pattern resembles jet flow, and hence, the airfoil is producing thrust.

### 3. Summary of force and efficiency data tests

The force and torque measurements of the pitching foil of saw-tooth angle of attack profile are taken as described in the previous section. The angular frequency  $\omega$  is kept constant while the pitch amplitude is varied from  $5^\circ$  to  $45^\circ$ . Figure 12 shows the experimentally measured values of (a) thrust coefficient,  $C_T$ , (b) power coefficient,  $C_P$ , and (c) efficiency,  $\eta$ , as a function of pitch amplitude,  $\theta_0$ . The principal results of the experiments are the following:

a)  $C_T$  increases with pitch amplitude,  $\theta_0$ , with the maximum value of 0.47 at  $\theta_0 = 45^\circ$  and  $St = 0.18$ . This shows that at this angular frequency ( $\omega = 0.698$  rad/s), higher pitch amplitude oscillations has resulted in larger thrust forces. At low Strouhal numbers ( $St < 0.2$ ), the corresponding increase in  $St$  also results in higher thrust forces

b)  $C_P$  increases with pitch amplitude,  $\theta_0$ , up to  $\theta_0 = 35^\circ$  before showing an unexpected decrease at  $\theta_0 = 40^\circ$  and  $45^\circ$ .

c) At constant angular frequency, efficiency values obtained are relatively low ( $\eta < 0.2$ ), except at  $\theta_0 = 5^\circ$  which showed an abnormally high value and was thus discarded. Efficiency values showed a slight decreasing trend up to  $\theta_0 = 35^\circ$  before increasing. The low efficiency values obtained may be attributed to the mismatching of the foil and wake parameters at small values of Strouhal number ( $St < 0.2$ ) and low angular frequency,  $\omega = 0.698$  rad/s. Larger pitching amplitude may yield more thrust but efficiency decreases as a result. Since the flow becomes more and more unsteady with increasing pitch amplitude and Strouhal number, the propulsive efficiency drops owing to a larger amount of vorticity shed from the trailing edge.

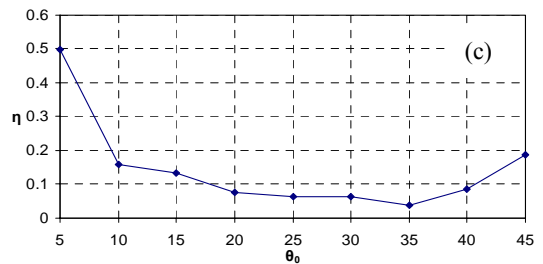
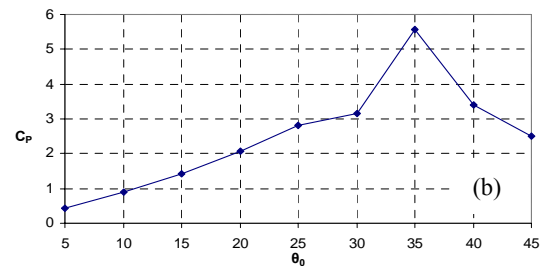
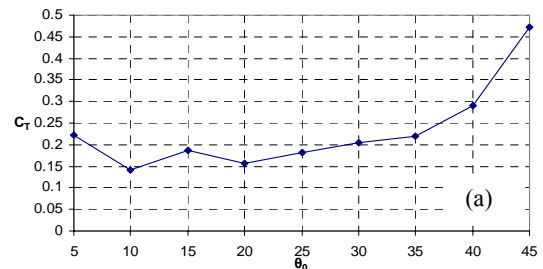


Fig. 12: (a) Thrust coefficient  $C_T$ , (b) power coefficient  $C_P$ , (c) efficiency  $\eta$ , as function of the pitch amplitude  $\theta_0$ .

Figure 13 shows the experimentally measured values of  $C_T$ ,  $C_P$ , and  $\eta$  as a function of angular frequency,  $\omega$ . In this set of experiments, the pitch amplitude was kept constant at  $\theta_0 = 10^\circ$

and the angular frequency was varied ( $0.393 < \omega < 3.14$  rad/s). The principal results of the experiments are:

a)  $C_T$  curve shows a slight increase up to a peak value of  $C_T = 1.14$  at  $St = 0.1$  and  $\omega = 1.57$  rad/s before dipping in value with further increase in  $St$  and  $\omega$ . At this low pitch amplitude of  $\theta_0 = 10^\circ$  and low Strouhal numbers ( $St < 0.2$ ), the increase in Strouhal number did not result in an increase in thrust force.

b)  $C_p$  coefficient curve showed a steady increase with corresponding increases in Strouhal number,  $St$ , and angular frequency,  $\omega$ .

c) The propulsive efficiency  $\eta$  shows a downward decreasing trend despite the increase in angular frequency. At a low pitch amplitude  $\theta_0 = 10^\circ$ , increasing the angular frequency did not improve efficiency at low Strouhal numbers. The rapid rise in  $C_p$  as  $St$  and  $\theta_0$  has resulted in the most of the decay in efficiency. Thus, at low Strouhal numbers, an increase in angular frequency resulted in a drop in efficiency. There is a mismatch between the foil and wake parameters even though high thrust forces are obtained at this pitch amplitude. The low efficiency values at this low Strouhal number makes it unsuitable for oscillating foil propulsion.

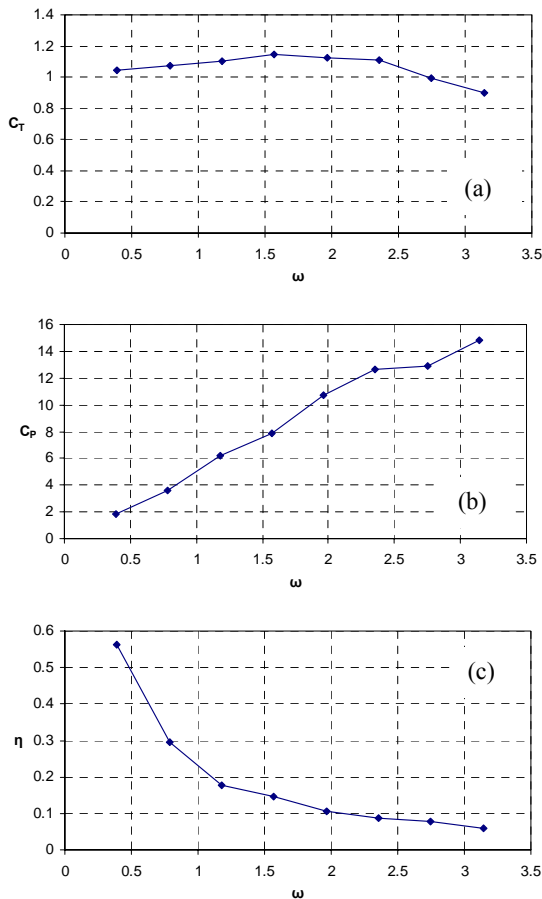


Fig. 13 (a) Thrust coefficient  $C_T$ , (b) power coefficient  $C_p$ , (c) efficiency  $\eta$ , as function of the angular frequency  $\omega$ .

Figure 14 shows the variation of the wake patterns with respect to  $St$ , which is plotted against the pitch amplitude  $\theta_0$  of the hydrofoil. In general, our results indicate that, at  $St < 0.2$ , the secondary, or vortex shedding mode dominates the flow, and the foil generates drag. As  $St$  increases, the influence of the flapping increases, and at a certain point the relative influence of both the flapping and the vortex shedding are balanced, and both vortex generating modes are phase-locked. This occurs approximately at  $0.2 < St < 0.55$ , and it appears that little or no net thrust or drag is developed. At  $St > 0.55$ , the flapping dominates the flow and the foil develops net thrust. Therefore, to maintain steady propulsion

the parameters of the flapping foil have to be chosen such that the thrust and drag are balanced. It is noted from the observation that steadily swimming fish swim approximately at  $St \approx 0.25$ .

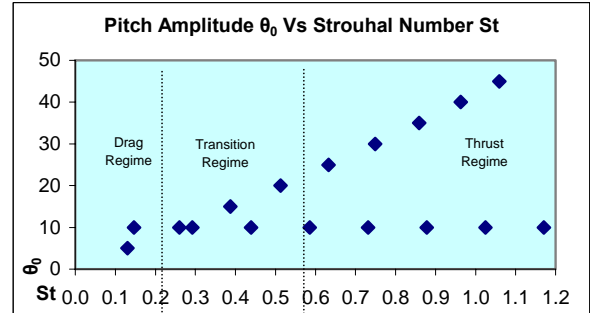


Fig. 14: Vortex jet or wake map ( $\diamond$  = collected data)

## Conclusion

It is found in this study that increasing pitch amplitude and angular frequency is associated with a decrease in propulsive efficiency and an increase in thrust forces produced. A high efficiency of 0.3 accompanied by a thrust coefficient of order one is found at a low pitch amplitude of  $10^\circ$  and angular frequency of 0.79 rad/s and Strouhal number of 0.05.

The dye flow visualisation experiments of the pitching foil has revealed different wake patterns at various Strouhal numbers. These wake patterns can be classified into three regimes – a drag regime, a transition regime and a thrust regime. The transition regime occurs at approximately  $0.2 < St < 0.55$ . Based on the wake regime, the Strouhal number for optimum propulsive efficiency must lie within this region.

## References

- Anderson, J. M., Streitlien, K., Barrett, D. S. and Triantafyllou, M. S., "Oscillating foils of high propulsive efficiency", *J. Fluid Mech.*, 360, 1998, 41–72.
- Barrett, D. S., Triantafyllou, M. S., Yue, D. K. P., Grosenbaugh, M. A. and Wolfgang, M. J., "Drag reduction in fish like locomotion", *J. Fluid Mech.*, 392, 1999, 183 – 212.
- Freymuth P., "Thrust generation by an airfoil in Hover modes," *Exp. Fluids*, Vol. 9, 1990, 17–24.
- Lighthill, M. J., "Aquatic animal propulsion of high hydrodynamical efficiency," *J. Fluid Mech.*, Vol. 44, No. 2, 1970, 265-301.
- Koochesfahani, M., "Vortical Patterns in the Wake of an Oscillating Airfoil," *AIAA Journal*, Vol. 27, No. 9, 1989, 1200-1205.
- McCroskey, W. J., "Some Current Research in Unsteady Fluid Dynamics," *J. Fluids Engineering*, Vol. 99, No. 1, 1977, 8-38.
- Muller, U. K., Stambhuis, E. J. and Videler, J. J., "Riding the waves: the role of the body wave in undulatory fish swimming", *Integrative and Comparative Biology*, 42, 2002, 981–987.
- Nakamura, Y., Vortex shedding from bluff bodies and a universal strouhal number, *J. Fluids and Struct.*, 10, 1996, 159–171.
- Ohashi H. and Ishikawa N., "Visualization study of flow near the trailing edge of an oscillating airfoil," *Bull. Jap. Soc. Mech. Engrng.*, Vol. 15, No. 85, 1972, 840–847.
- Poling D. R. and Telionis D. P., "The trailing edge of a pitching airfoil at high reduced frequencies," *J. Fluids Eng.*, Vol. 109, 1987, 410–414.
- Schultz, W. W. and Webb, P. W., "Power requirements of swimming: Do new methods resolve old questions?", *Integrative and Comparative Biology*, 42, 2002, 1018 – 1025.
- Triantafyllou G. S., Triantafyllou M. S., and Grosenbaugh M. A., "Optimal thrust development in oscillating foils with application to fish propulsion," *J. Fluids Struct.*, Vol. 7, 1993, 205–224.
- Triantafyllou, M. S., Triantafyllou, G. S., and Gopalkrishnan R., "Wake mech. for thrust generation in oscillating foils," *Phys. Fluids*, Vol. 3, No. 12, 1991, 2835–2837.
- Triantafyllou, M. S., Techet, A. H., Zhu, Q., Beal, D. N., Hover, F. S. and Yue, D. K. P., "Vorticity control in fish-like propulsion and maneuvering", *Integrative and Comparative Biology*, Vol. 42, 2002, 1026–1031.
- Triantafyllou, M. S., Triantafyllou, G. S. and Yue, D. K. P., "Hydrodynamics of fishlike swimming", *Annual Review of Fluid Mechanics* 32 2000 33 – 53